DOR:

Research Paper

Effect of Welding Processing Parameters on FSW of Aerospace Grade Aluminum Alloys

Erfan Khosravian[1*]
[1]Department of Mechanical Engineering, Payam Noor University, Tehran, Iran
[*]Email of the Corresponding Author: erfankhosravian1994@gmail.com
Received: February 12, 2024; Accepted: April 23, 2024

Abstract
This study aimed to investigate the influence of rotational and traverse speeds on the friction stir welding (FSW) of aerospace-grade aluminum alloys. To achieve this, a thermo-mechanically coupled 3D finite element analysis (FEM) was employed to analyze the impact of these speeds on temperature and strain. Additionally, tensile tests were conducted on welded joints fabricated using varying tool rotational and traverse speeds to examine the effects of welding speed on the tensile properties of the specimens. The results revealed that high welding speeds had a detrimental effect on the mechanical properties of the weld samples. Samples produced using an optimal rotational speed of 1200 rpm and a traverse speed of 40 mm exhibited a tensile strength of 346 MPa, which accounts for approximately 64% of the strength seen in the base material.

Keywords
FSW, Rotational Speed, Traverse Speed, Tensile, FEM

1. Introduction

Friction Stir Welding (FSW) is a revolutionary joining technique that has transformed the welding industry [1,2]. Unlike traditional welding methods that involve melting and solidification, FSW uses frictional heat and mechanical deformation to create strong, defect-free welds [3]. By operating at lower temperatures, FSW preserves the desirable properties of the materials being joined, resulting in improved strength, fatigue resistance [4,5], and corrosion properties [6,7]. FSW's versatility in joining materials such as aluminum [8,9], copper [10,12], and steel alloys has made it a popular choice across various industries, including aerospace, automotive, and shipbuilding.

FSW has emerged as a game-changing technique for joining aerospace-grade aluminum alloys, such as the commonly used 2xxx, 6xxx, and 7xxx series [13-15]. These alloys are known for their high strength-to-weight ratio and excellent corrosion resistance, making them ideal for aerospace applications. FSW offers several advantages when welding these aluminum alloys. Firstly, the process operates at lower temperatures, minimizing distortion and preserving the desirable mechanical properties of the materials. This is crucial in maintaining the structural integrity of aircraft components. Secondly, FSW eliminates the need for filler materials, resulting in welds with reduced porosity and improved fatigue resistance, which are critical for the long-term performance and reliability of aerospace structures [16]. Moreover, FSW's solid-state nature avoids the formation of

solidification defects, ensuring defect-free welds with enhanced joint strength [17,18]. The capability of FSW to join dissimilar aluminum alloys, such as those with varying strength or thermal properties, further expands design possibilities and enables the creation of lightweight and efficient aerospace structures [19-21]. By offering high-quality welds and meeting the stringent requirements of the aerospace industry, FSW has become a preferred choice for joining aerospace-grade aluminum alloys and is contributing to the advancement of aerospace manufacturing. Kumar et al. [22] explored the friction stir welding (FSW) process to create strong metallurgical bonds in 6061 and 7075 Al alloys by employing intense deformations and heat from friction. Their study highlighted the critical role of selecting optimal welding parameters, like rotational speed, tool tilt angle, and axial force, to enhance joint quality. Experiments conducted on twenty-seven alloy joints emphasized variations in mechanical properties such as tensile strength, impact strength, and hardness, affecting welding conditions. Anandan and Manikandan [23] examined the effects of welding speeds on friction stir welding of aluminum alloys, finding that 65 mm/min produced optimal mechanical properties due to finer grain structure and better material mixing, resulting in superior tensile strength. Lewise and Dhas [24] explored friction stir spot welding of AA2024 and AA7075 aluminum alloys using the Box-Behnken design of response surface methodology. Their research confirmed the chemical composition via XRD analysis and identified tool rotation speed as a key parameter influencing tensile shear force, which improved with optimized welding settings. The study validated the desirability approach in predicting optimal tensile shear values, supported by consistent microstructural analyses. Kumar et al. [25] optimized friction stir welded joints of AA7050 and AA6082 alloys using response surface methodology, analyzing the effects of tool tilt angle, rotational speed, and welding speed on tensile strength, strain, and hardness. They found optimal mechanical properties at specific settings, with sub-grain formation crucial for enhancing toughness.

The rotational and traverse speeds are crucial parameters in determining the quality and characteristics of FSW joints [26,27]. The rotational speed determines the frictional heat generated, softening the material and facilitating plastic deformation [28]. Higher rotational speeds increase heat generation, leading to better material flow and improved joint formation. However, excessively high rotational speeds can cause material defects and excessive tool wear [29]. On the other hand, lower rotational speeds may lead to insufficient heat generation, resulting in inadequate material flow and weak welds. The traverse speed affects the residence time of the tool in a particular region. Higher traverse speeds reduce the heat input, which can lead to incomplete mixing and weak bonding. Slower traverse speeds allow more time for material mixing, resulting in better weld integrity. However, excessively slow traverse speeds can cause excessive heat input, leading to material defects such as tunneling and voids [30]. Therefore, finding the optimal balance between rotational and traverse speeds is crucial for achieving defect-free, high-quality welds in FSW [31]. The selection of these parameters depends on various factors, such as the material being welded, joint geometry, and desired weld properties. Through careful control and optimization of rotational and traverse speeds, engineers can achieve optimal material flow, heat distribution, and mechanical properties, ensuring the successful application of FSW in various industries [32].

Simulation plays a vital role in advancing FSW processes by providing valuable insights and optimizing weld quality [33-35]. FSW simulations utilize computational models to predict the behavior of materials and the welding process itself. These simulations help engineers understand the

complex thermo-mechanical interactions occurring during FSW, allowing for the optimization of process parameters, tool design, and material selection [36]. By simulating FSW, engineers can assess the temperature distribution, material flow, and residual stresses within the weld region, enabling them to identify potential defects and optimize the welding parameters to mitigate their occurrence [37-39]. Additionally, simulations aid in predicting the microstructural evolution and mechanical properties of the weld, providing valuable information for assessing the long-term performance and durability of the joint [40-42]. Furthermore, virtual simulations enable the exploration of different welding scenarios and design variations, leading to improved process efficiency, reduced development time, and cost savings.

The study you described aimed to investigate how the speed of rotational and traverse speeds in FSW affect the welding of aerospace-grade aluminum alloys. To analyze the influence of rotational and traverse speed on FSW, the researchers employed a 3D finite element analysis (FEM). Additionally, the study conducted tensile tests on welded joints created with different tool speeds. By examining the tensile properties of the specimens, the researchers aimed to understand how the welding speed affected the strength and integrity of the welds.

2. Experimental method

Experiments were performed on rolled plates of AA7075-O aluminum alloys of 5 mm thickness, which have chemical compositions as given in Table 1.

Table 1. Chemical composition of AA7075-O aluminum alloys (wt%)

Si	Fe	Mn	Cu	Zn	Ti	Mg
0.27	0.36	0.02	1.2	4.7	0.03	1.74

The different tool rotational speeds of 800, 1200, and 1600 rpm and traverse speeds of 20, 40, and 60 mm/min were used to investigate the effects of tool traverse and rotational speeds. The H13 steel FSW tool consists of a cylindrical inserted pin with a 5 mm diameter, 4 mm height, and a 15 mm shoulder diameter (Figure 1) and rotated with a constant tilt angle of 3º, which helps in forging action at the trailing edge of the shoulder [43-45]. The penetration depth of the tool into the material was approximately 1 mm from the top of the pin.

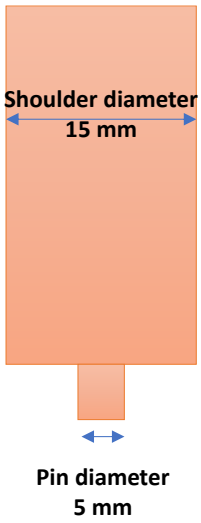

Figure 1. The dimensions of the tool used in this research

To obtain tensile specimens, the welded joints were first sliced using a power hacksaw and then machined to the necessary dimensions. The preparation of smooth and notched tensile specimens followed the guidelines outlined in ASTM E8 M-04, and the specific dimensions can be seen in Figure 2. The tensile test was conducted at room temperature using a universal testing machine. The test was performed with a cross-head speed of 1 mm/min.

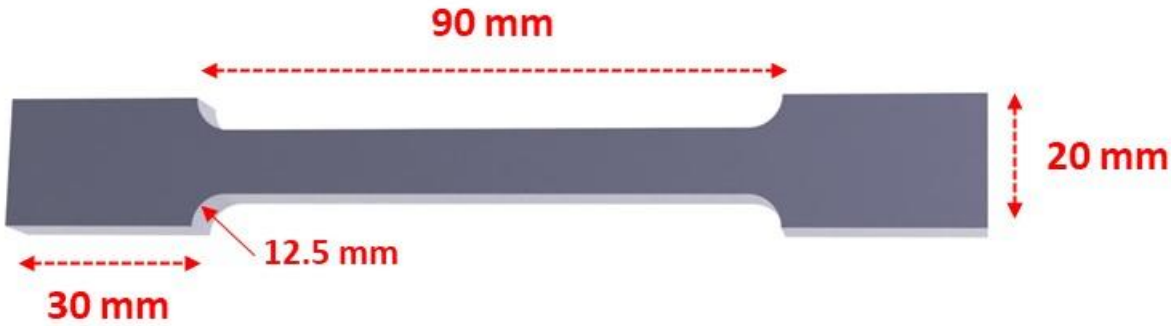

Figure 2. The specific dimensions of tensile specimens

3. Simulation details

To simulate the temperature and strain during the friction stir process under different welding speeds, the researchers utilized Deform-3D^{TM} software [46]. To simulate the process numerically, a 3D FEM analysis incorporating thermo-mechanical coupling was employed. In this study, the FSW tool was treated as a rigid body and was meshed using tetrahedral elements. The workpiece was divided into multiple zones and meshed with different element sizes. To enhance simulation accuracy, smaller elements with a mean length of 0.7 mm were placed in proximity to the FSW tool (as shown in Figure 3).

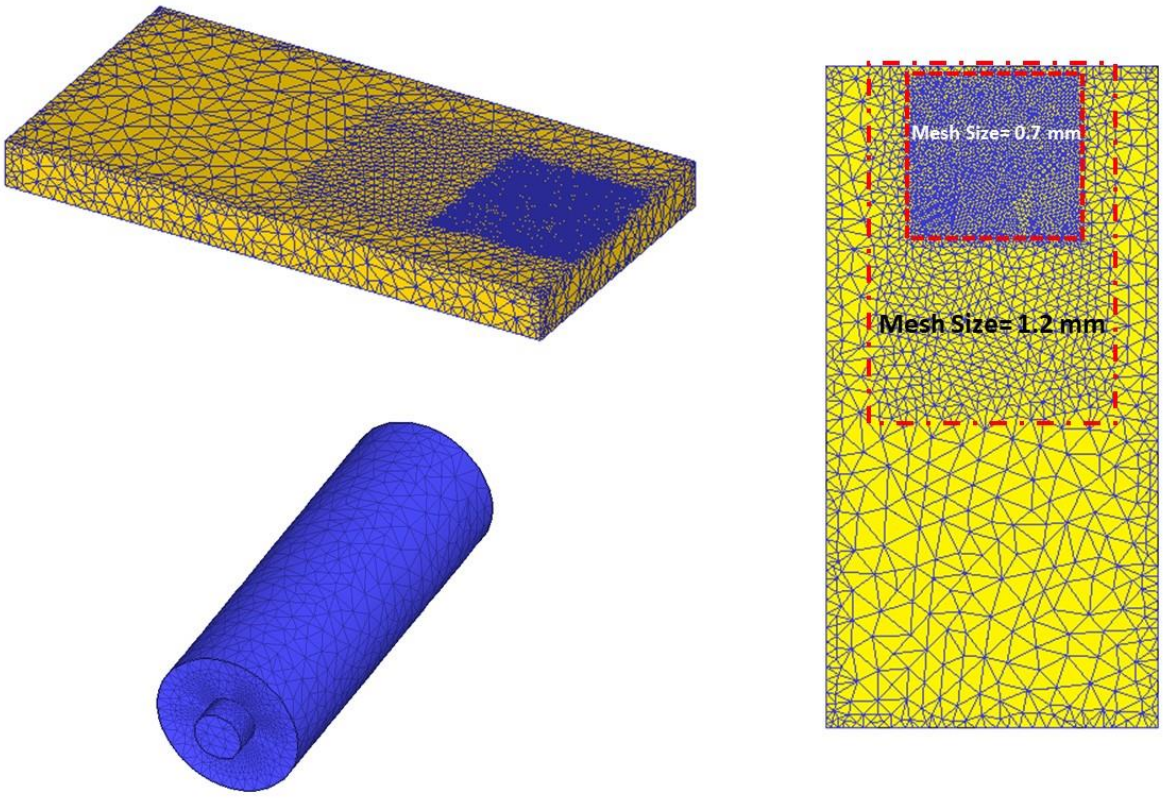

Figure 3. Illustration of the workpiece and the FSW tool

The relationship between the flow stress of AA7075 aluminum alloy and various factors, including strain rate, temperature, and plastic strain, is established as follows [47,48]:

$$\bar{\sigma} = \bar{\sigma}(\bar{\varepsilon}, \dot{\bar{\varepsilon}}, \mathrm{T}) \qquad (1)$$

Where $\bar{\sigma}$, $\bar{\varepsilon}$, $\dot{\bar{\varepsilon}}$ and T represent the plastic strain, the strain rate, the flow, and the temperature, respectively.

This study employs a constant shear friction model to represent the friction between the tool and the workpiece. The frictional force can be determined using the following equation in this model. [48]:

$$f = mk \qquad (2)$$

The variables f, k, and m in the equation represent the frictional stress at the interface between the tool and workpiece, the shear yield stress, and the shear friction factor, respectively. The convective boundary condition for all surfaces of the weldment is specified as follows:

$$k\frac{\partial T}{\partial n} = h(T - T_{amb}) \qquad (3)$$

The convective boundary condition is defined by the equation mentioned, where h denotes the convection coefficient, T_{amb} represents the ambient temperature, and n represents the normal vector of the boundary. In this study, the convection coefficient for the surfaces of the welded sample exposed to the environment is assumed to be 20 W/(m^2.ºC). Additionally, the thermal properties of the H13 steel tool and AA7075 samples are provided in Table 2.

Table 2. Thermal properties of the AA7075 aluminum alloy and H13 FSW tool

Property	AA7075	FSW Tool
Conductivity (W/m ^{o}C)	130	24.5
Heat transfer coefficient between tool and billet (N /^{o}C s mm^{2})	11	11
Heat transfer coefficient between the backing plate and billet (N/ ^{o}C s mm^{2})	5	

4. Result and discussion

4.1 Effect of process parameters on the temperature history

In FSW, temperature plays a critical role in the welding process. During FSW, a rotating tool with a specially designed geometry is plunged into the workpiece, generating frictional heat as it moves along the joint line. This heat softens the material, allowing the tool to stir the plasticized metal and create a strong bond. Various factors, including the rotational speed of the tool, the welding speed, the tool geometry, and the material properties, influence the temperature in FSW. As the tool rotates and moves along the joint line, it generates heat due to the friction between the tool and the workpiece. The temperature can rise significantly, reaching temperatures close to the recrystallization temperature of the material [49].

Controlling the temperature in FSW is crucial to ensure the quality of the weld. Excessive heat can lead to defects such as material degradation, excessive grain growth, and even metallurgical changes. On the other hand, insufficient heat can result in incomplete bonding and weak joints. Therefore, precise temperature control is necessary to achieve optimal weld integrity.

Figures 4 and 5 show the temperature profile along the transverse section of the weld zone for different rotational speeds. It is observed from this figure that temperature distribution about the weld line is nearly symmetric for all rotational speeds. This is in line with the results reported by Buffa et al. [50]. They stated that the temperature profile along a transverse section is symmetric because the heat generation during FSW is dominated by the tool rotating speed which is much higher than the traverse speed.

This figure shows that a higher temperature value can be seen with increasing tool rotational speed. Increasing rotational speed from 800 to 1600 rpm increased the peak temperature observed in SZ from 350 C to 450 C. The higher temperature value in the FSW joint is favorable for solid diffusion and plasticized mixing and, hence, is helpful for weld quality in terms of material flow. On the other hand, excessive speeds may result in defects that compromise the mechanical properties. Therefore, an optimum rotational speed exists that provides a high peak temperature in the weld zone and doesn't produce defects.

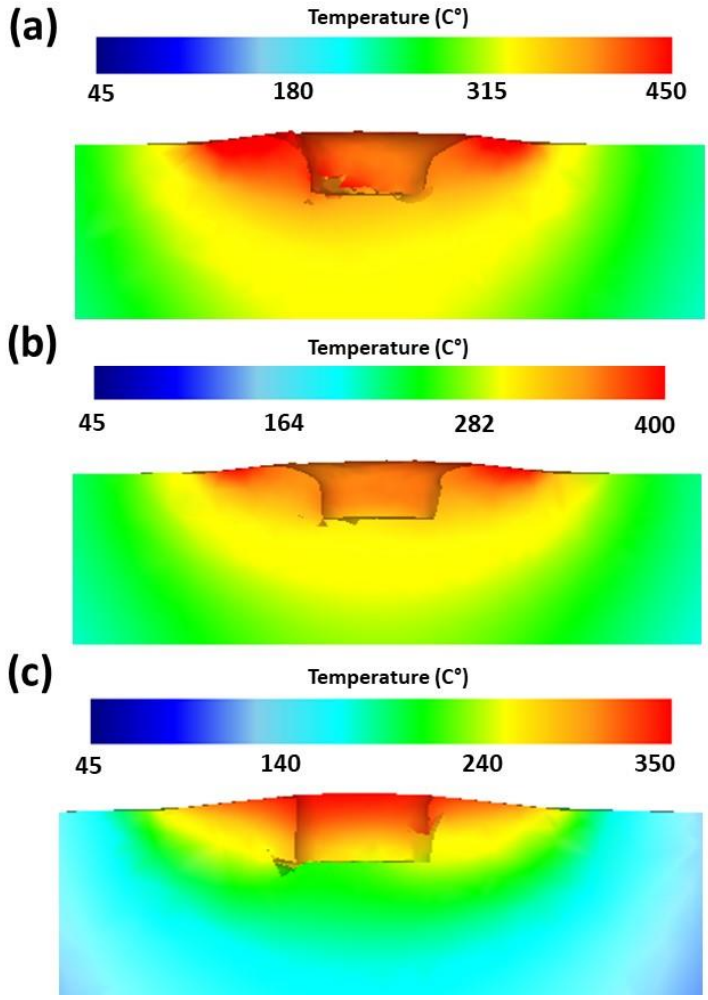

Figure 4. Temperature profile along the transverse section of the weld zone for different rotational speeds of a) 800 rpm, b) 1200 rpm, and c) 1600 rpm

Figure 5 illustrates the temperature distribution across the transverse section of the weld zone at various traverse speeds. It is evident from the figure that as the tool traverse speed decreases, higher temperature values are observed. This temperature increase can be primarily attributed to the extended time required to heat up and weld the same length of the material.

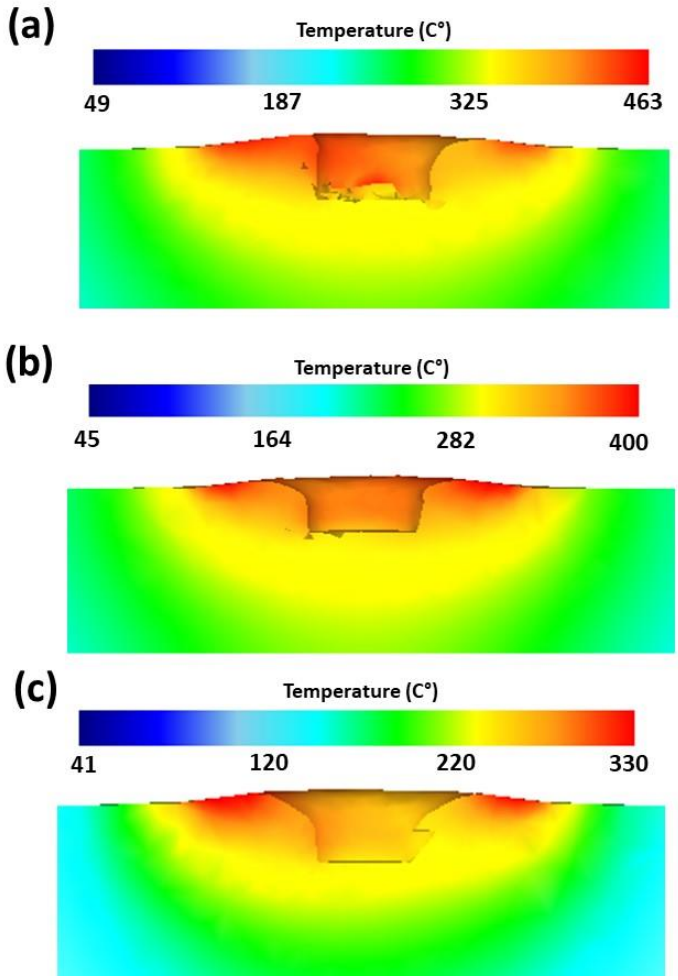

Figure 5. Temperature profile along the transverse section of the weld zone for different traverse speeds of a) 20 mm/min, b) 40 mm/min, and c) 60 mm/min

4.2 Effect of process parameters on the strain history

Strain plays a significant role in FSW as it directly affects the deformation and mechanical properties of the welded joint. During the FSW process, the rotating tool generates frictional heat, which softens the material and induces plastic deformation. As the tool moves along the joint line, it creates a plasticized zone where the material undergoes severe plastic strain. This plastic strain causes material flow, mixing, and consolidation, resulting in the formation of a solid-state weld. The amount and distribution of strain in the weld region influence the microstructure, grain size, and texture, which in turn affect the mechanical properties of the joint. Excessive strain can lead to material defects such as voids, tunneling, or cracks, compromising the integrity of the weld. Therefore, careful control and optimization of process parameters, such as rotational and traverse speeds, can help regulate the strain levels and ensure the production of high-quality, defect-free welds with desirable mechanical properties in FSW [51].

Figures 6 and 7 present the strain distribution observed during FSW while employing different combinations of rotational and traverse speeds. The strain distribution around the weld line displays asymmetry, as depicted in the figures. Additionally, the affected region experiences a greater extent

of strain on the advancing side, indicating a positive relationship between traverse speed and tool rotational speed [52].

The figures demonstrate that as rotational speed increases or traverse speed decreases, both the maximum strain and the area subjected to plastic deformation increase. This phenomenon can be attributed to the generation of additional heat, leading to heightened material softening. Consequently, an enlarged nugget zone is formed as a result of the increased maximum strain and plastically deformed area [53].

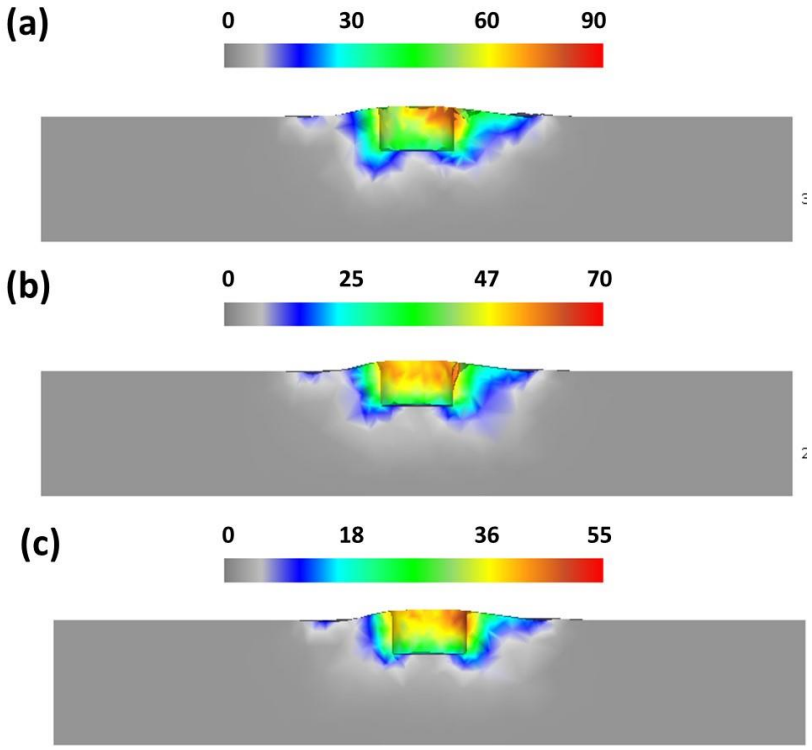

Figure 6. Strain profile along the transverse section of the weld zone for different rotational speeds of a) 800 rpm, b) 1200 rpm, and c) 1600 rpm

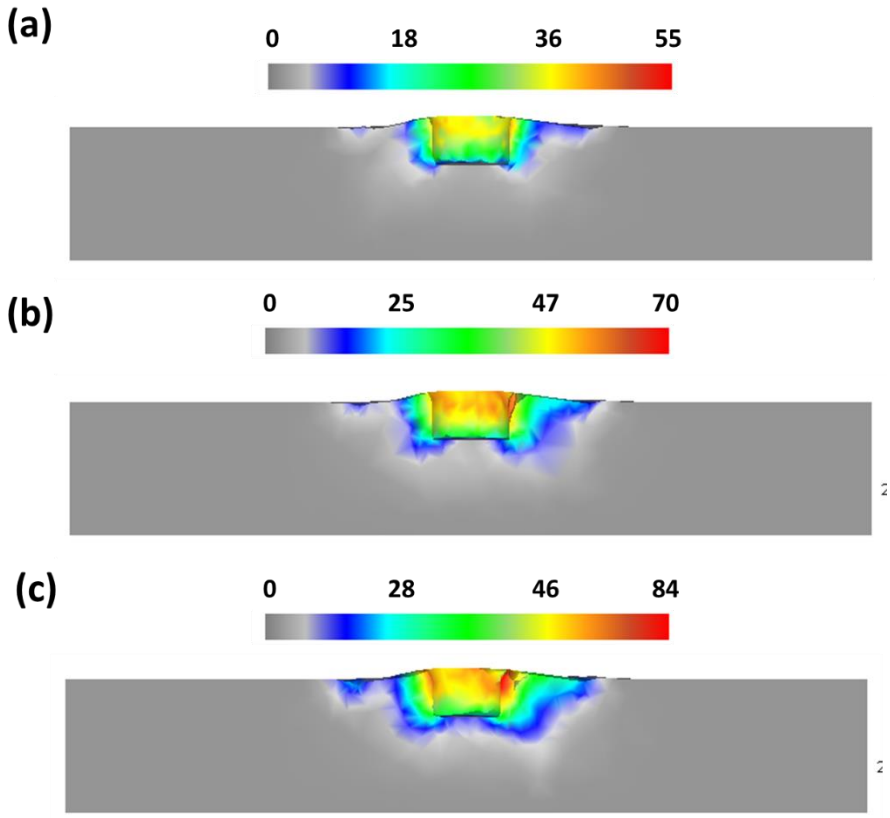

Figure 7. Strain profile along the transverse section of the weld zone for different rotational speeds of a) 800 rpm, b) 1200 rpm, and c) 1600 rpm

4.3. Effect of process parameters on the tensile test

The welding speed is a significant parameter that influences the amount of heat generated in the FSW process. During welding, the stirring zone experiences substantial plastic deformation and high heat input that leads to recrystallization within the stirring zone and dissolution and coarsening of the precipitation around it. These microstructural changes in the affected zones impact both the microstructure of the bond after welding and mechanical characteristics like hardness and tensile strength. By utilizing optimal welding parameters, including rotational speed and traverse speed, in FSW processes, it is possible to achieve welded joints with the most favorable mechanical properties [13,53].

Figure 8 presents the tensile properties of the welded specimens produced at different rotational and traverse speeds. Tensile tests were conducted on the base material, revealing a tensile strength of 540 MPa. The results of the tensile tests indicated that the highest weld efficiency was attained with the specimen produced at a welding speed of 1200 rpm. Also, the traverse speed of 40 mm/min results in the welded sample with the highest tensile strength compared to other traverse speeds. The tensile strength of samples produced by an optimum rotational speed of 1200 rpm and traverse speed of 40 mm is 346 MPa, about 64% of base material strength.

Additionally, the welded joints are typically fractured close to the weld center [54]. The results show that the tool rotational speed and traverse speed in FSW profoundly influence the tensile properties of welded specimens [55]. The rotational and traverse speed determines the heat generation, plastic deformation, grain refinement, and defect formation during welding. Higher welding speeds generate

more heat, promote intense stirring and mixing, and can lead to finer grain structures. However, excessive speeds may result in defects that compromise the tensile properties [56].

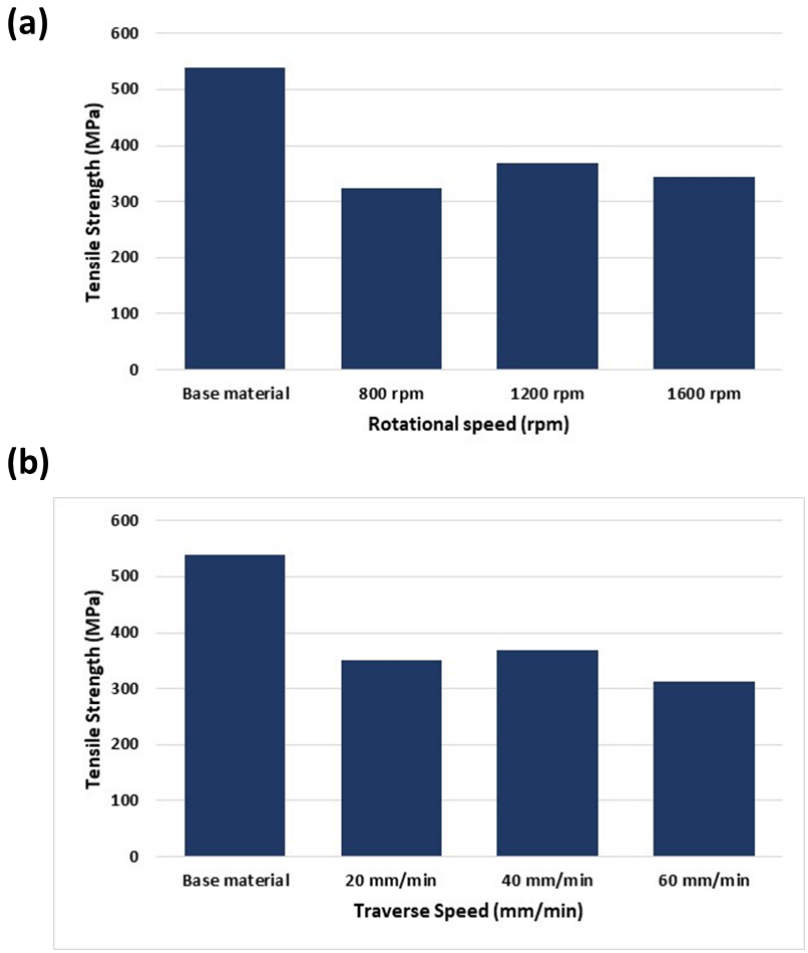

Figure 8. The tensile properties of the welded specimens produced at a) different rotational and b) traverse speeds

5. Conclusion

This study employed a 3D FEM analysis that integrated thermomechanical coupling to explore the impact of rotational and traverse speeds on strain and temperature. Furthermore, the researchers performed tensile tests on welded joints created with different tool rotational and traverse speeds to assess how welding speed influences the tensile properties of the specimens. The findings of this investigation can be summarized as follows:

- It was observed that increasing the tool rotational speed resulted in higher temperature values while decreasing the tool traverse speed also led to higher temperatures due to the prolonged heating and welding time required for the same length of material.
- The tensile tests conducted on the welded joints indicated that the specimen produced at a welding speed of 1200 rpm exhibited the highest weld efficiency. Additionally, among the various traverse speeds tested, a traverse speed of 40 mm/min resulted in the welded sample with the highest tensile strength compared to other traverse speeds.
- Elevating the rotational speed from 800 to 1600 rpm resulted in a rise in the maximum temperature recorded in the SZ, ascending from 350°C to 450°C.

Samples fabricated utilizing an optimal rotational velocity of 1200 rpm and a traverse speed of 40 mm showcase a tensile strength of 346 MPa. This magnitude of strength corresponds to approximately 64% of the tensile strength exhibited by the base material.

6. References

[1] Mishra, R.S. and Ma, Z. 2005. Friction stir welding and processing. Materials Science and Engineering: R: Reports. 50:1-78. doi:10.1016/j.mser.2005.07.001.

[2] HajimohamadzadehTorkambour, S., Nejad, M.J., Pazoki, F., Karimi, F. and Heydari, A. 2024. Synthesis and characterization of a green and recyclable arginine-based palladium/CoFe2O4 nanomagnetic catalyst for efficient cyanation of aryl halides. RSC Advances. 14(20):14139-14151. doi:10.1039/D4RA01200C.

[3] Kumar Rajak, D., Pagar, D.D., Menezes, P.L. and Eyvazian, A. 2020. Friction-based welding processes: friction welding and friction stir welding. Journal of Adhesion Science and Technology. 34:2613-2637. doi:10.1080/01694243.2020.1780716.

[4] Fratini, L. and Pasta, S. 2005. Fatigue resistance of AA2024-T4 friction stir welding joints: influence of process parameters. Structural Durability & Health Monitoring. 1:245. doi:10.3970/sdhm.2005.001.245.

[5] Costa, J., Ferreira, J. and Borrego, L. 2011. Influence of spectrum loading on fatigue resistance of AA6082 friction stir welds. International Journal of Structural Integrity. 2:122-134. doi:10.1108/17579861111135888.

[6] Lumsden, J., Mahoney, M., Rhodes, C. and Pollock, G. 2003. Corrosion behavior of friction-stir-welded AA7050-T7651. Corrosion. 59. doi:10.5006/1.3277553.

[7] Moreto, J., Dos Santos, M., Ferreira, M., Carvalho, G., Gelamo, R., Aoki, I.V., Taryba, M., Bose Filho, W.W. and Fernandes, J. 2021. Corrosion and corrosion-fatigue synergism on the base metal and nugget zone of the 2524-T3 Al alloy joined by FSW process. Corrosion Science. 182:109253. doi:10.1016/j.corsci.2021.109253.

[8] Chien, C.-H., Lin, W.-B. and Chen, T. 2011. Optimal FSW process parameters for aluminum alloys AA5083. Journal of the Chinese Institute of Engineers. 34:99-105. doi:10.1080/02533839.2011.553024.

[9] Su, J.-Q., Nelson, T.W. and Sterling, C.J. 2005. Microstructure evolution during FSW/FSP of high strength aluminum alloys. Materials Science and Engineering: A. 405:277-286. doi:10.1016/j.msea.2005.06.009.

[10] Lee, W.-B. and Jung, S.-B. 2004. The joint properties of copper by friction stir welding. Materials Letters. 58:1041-1046. doi:10.1016/j.matlet.2003.08.014.

[11] Sakthivel, T. and Mukhopadhyay, J. 2007. Microstructure and mechanical properties of friction stir welded copper. Journal of Materials Science. 42:8126-8129. doi:10.1007/s10853-007-1666-y.

[12] Eslami, N., Hischer, Y., Harms, A., Lauterbach, D. and Böhm, S. 2019. Optimization of process parameters for friction stir welding of aluminum and copper using the taguchi method. Metals. 9:63. doi:10.3390/met9010063.

[13] Ahmed, M.M., El-Sayed Seleman, M.M., Fydrych, D. and Çam, G. 2023. Friction stir welding of aluminum in the aerospace industry: The current progress and state-of-the-art review. Materials. 16:2971. doi:10.3390/ma16082971.

[14] Prater, T. 2014. Friction stir welding of metal matrix composites for use in aerospace structures. Acta Astronautica. 93:366-373. doi:10.1016/j.actaastro.2013.07.023.

[15] Mishra, A. and Dixit, D. 2018. Friction stir welding of aerospace alloys. Journal of Mechanical Engineering. 48:37-46.

[16] Omer, M.A., Rashad, M., Elsheikh, A.H. and Showaib, E.A. 2022. A review on friction stir welding of thermoplastic materials: Recent advances and progress. Weld World. 1-25. doi:10.1007/s40194-021-01178-0.

[17] Akbari, M., Rahimi Asiabaraki, H., Hassanzadeh, E. and Esfandiar, M. 2023. Simulation of dissimilar friction stir welding of AA7075 and AA5083 aluminium alloys using Coupled Eulerian–Lagrangian approach. Welding International. 37:174-184. doi:10.1080/09507116.2023.2205035.

[18] Shahnazari, M.R. and Esfandiar, M. 2018. Capillary Effects on Surface Enhancement in a Non-Homogeneous Fibrous Porous Medium. Mechanics of Advanced Composite Structures. 5:83-90. doi:10.22075/macs.2017.1558.1074.

[19] Sambasivam, S., Gupta, N., Singh, D.P., Kumar, S., Giri, J.M. and Gupta, M. 2023. A review paper of FSW on dissimilar materials using aluminum. Materials Today: Proceedings (In Press). doi:10.1016/j.matpr.2023.03.304.

[20] Saadati, S. and Esfandiar, M. 2020. Partial and full β-bromination of meso-tetraphenylporphyrin: Effects on the catalytic activity of the manganese and nickel complexes for photo oxidation of styrene in the presence of molecular oxygen and visible light. Journal of Organometallic Chemistry. 924:121464. doi:10.1016/j.jorganchem.2020.121464.

[21] Esfandiar, M., Nikan, F. and Shahnazari, M.R. 2017. Catalytic pyrolysis of coal particles in a fluidized bed: Experiments and modeling. Energy Sources, Part A: Recovery, Utilization, and Environmental Effects. 39:1478-1483. doi:10.1080/15567036.2016.1278488.

[22] Seshu Kumar, G., Kumar, A., Rajesh, S., Chekuri, R.B.R. and Ramakotaiah, K. 2023. An experimental study and parameter optimization of FSW for welding dissimilar 6061 and 7075 Al alloys. International Journal on Interactive Design and Manufacturing. 17:215-223. doi:10.1007/s12008-022-00913-1.

[23] Anandan, B. and Manikandan, M. 2023. Effect of welding speeds on the metallurgical and mechanical property characterization of friction stir welding between dissimilar aerospace grade 7050 T7651-2014A T6 aluminium alloys. Materials Today Communications. 35:106246. doi:10.1016/j.mtcomm.2023.106246.

[24] Anton Savio Lewise, K. and Edwin Raja Dhas, J. 2022. FSSW process parameter optimization for AA2024 and AA7075 alloy. Materials and Manufacturing Processes. 37:34-42. doi:10.1080/10426914.2021.1962532.

[25] Kumar, J., Kumar, G., Mehdi, H. and Kumar, M. 2023. Optimization of FSW parameters on mechanical properties of different aluminum alloys of AA6082 and AA7050 by response surface methodology. International Journal on Interactive Design and Manufacturing. 18:1359–1371. doi: doi:10.1007/s12008-023-01425-2.

[26] Bijanrostami, K., Barenji, R.V. and Hashemipour, M. 2017. Effect of traverse and rotational speeds on the tensile behavior of the underwater dissimilar friction stir welded aluminum alloys. Journal of Materials Engineering and Performance. 26:909-920. doi:10.1007/s11665-017-2506-0.

[27] Bilgin, M.B. and Meran, C. 2012. The effect of tool rotational and traverse speed on friction stir weldability of AISI 430 ferritic stainless steels. Materials & Design. 33:376-383. doi:10.1016/j.matdes.2011.04.013.

[28] Khan, N.Z. and Bajaj, D., Siddiquee, A.N., Khan, Z.A., Abidi, M.H., Umer, U. and Alkhalefah, H. 2019. Investigation on effect of strain rate and heat generation on traverse force in FSW of dissimilar aerospace grade aluminium alloys. Materials. 12:1641. doi:10.3390/ma12101641.

[29] Salari, E., Jahazi, M., Khodabandeh, A. and Ghasemi-Nanesa, H. 2014. Influence of tool geometry and rotational speed on mechanical properties and defect formation in friction stir lap welded 5456 aluminum alloy sheets. Materials & Design. 58:381-389. doi:10.1016/j.matdes.2014.02.005.

[30] Zhao, Y., Han, J., Domblesky, J.P., Yang, Z., Li, Z. and Liu, X. 2019. Investigation of void formation in friction stir welding of 7N01 aluminum alloy. Journal of Manufacturing Processes. 37:139-149. doi:10.1016/j.jmapro.2018.11.019.

[31] Asadi, P., Aliha, M.R.M., Akbari, M., Imani, D.M. and Berto, F. 2022. Multivariate optimization of mechanical and microstructural properties of welded joints by FSW method. Engineering Failure Analysis. 140:106528. doi:10.1016/j.engfailanal.2022.106528.

[32] Akbari, M. and Rahimi Asiabaraki, H. 2023. Modeling and optimization of tool parameters in friction stir lap joining of aluminum using RSM and NSGA II. Welding International. 37:21-33. doi:10.1080/09507116.2022.2164530.

[33] Dialami, N., Chiumenti, M., Cervera, M., Segatori, A. and Osikowicz, W. 2017. Enhanced friction model for Friction Stir Welding (FSW) analysis: Simulation and experimental validation. International Journal of Mechanical Sciences. 133:555-567. doi:10.1016/j.ijmecsci.2017.09.022.

[34] Sibalic, N. and Vukcevic, M. 2019. Numerical simulation for FSW process at welding aluminium alloy AA6082-T6. Metals. 9:747. doi:10.3390/met9070747.

[35] Eskandari, E., Alimoradi, H., Pourbagian, M. and Shams, M. 2022. Numerical investigation and deep learning-based prediction of heat transfer characteristics and bubble dynamics of subcooled flow boiling in a vertical tube. Korean Journal of Chemical Engineering. 39:3227-3245. doi:10.1007/s11814-022-1267-0.

[36] Guerdoux, S. and Fourment, L. 2009. A 3D numerical simulation of different phases of friction stir welding. Modelling and Simulation in Materials Science and Engineering. 17:075001. doi:10.1088/0965-0393/17/7/075001.

[37] Zhu, Y., Chen, G., Chen, Q., Zhang, G. and Shi, Q. 2016. Simulation of material plastic flow driven by non-uniform friction force during friction stir welding and related defect prediction. Materials & Design. 108:400-410. doi:10.1016/j.matdes.2016.06.119.

[38] Türkan, M. and Karakaş, Ö. 2022. Numerical modeling of defect formation in friction stir welding. Materials Today Communications. 31:103539. doi:10.1016/j.mtcomm.2022.103539.

[39] Dialami, N., Cervera, M. and Chiumenti, M. 2020. Defect formation and material flow in friction stir welding. European Journal of Mechanics-A/Solids. 80:103912. doi:10.1016/j.euromechsol.2019.103912.

[40] Grujicic, M., Ramaswami, S., Snipes, J., Avuthu, V., Galgalikar, R. and Zhang, Z. 2015. Prediction of the grain-microstructure evolution within a Friction Stir Welding (FSW) joint via the

use of the Monte Carlo simulation method. Journal of Materials Engineering and Performance. 24:3471-3486. doi:10.1007/s11665-015-1635-6.

[41] Dialami, N., Cervera, M. and Chiumenti, M. 2018. Numerical modelling of microstructure evolution in friction stir welding (FSW). Metals. 8:183. doi:10.3390/met8030183.

[42] Alimoradi, H., Eskandari, E., Pourbagian, M. and Shams, M. 2022. A parametric study of subcooled flow boiling of Al2O3/water nanofluid using numerical simulation and artificial neural networks. Nanoscale and Microscale Thermophysical Engineering. 26(2–3):129–159. doi:10.1080/15567265.2022.2108949.

[43] Khodaverdizadeh, H., Mahmoudi, A., Heidarzadeh, A. and Nazari, E. 2012. Effect of friction stir welding (FSW) parameters on strain hardening behavior of pure copper joints. Materials & Design. 35:330-334. doi:10.1016/j.matdes.2011.09.058.

[44] Koilraj, M., Sundareswaran, V., Vijayan, S. and Koteswara Rao, S.R. 2012. Friction stir welding of dissimilar aluminum alloys AA2219 to AA5083 – Optimization of process parameters using Taguchi technique. Materials & Design. 42:1-7. doi:10.1016/j.matdes.2012.02.016.

[45] Radisavljevic, I., Zivkovic, A., Radovic, N. and Grabulov, V. 2013. Influence of FSW parameters on formation quality and mechanical properties of Al 2024-T351 butt welded joints. Transactions of Nonferrous Metals Society of China, 23:3525-3539. doi: 10.1016/S1003-6326(13)62897-6.

[46] Akbari, M., Aliha, M.R.M. and Berto, F. 2023. Investigating the role of different components of friction stir welding tools on the generated heat and strain. Forces in Mechanics. 10:100166. doi:10.1016/j.finmec.2023.100166.

[47] Asadi, P., Mahdavinejad, R.A. and Tutunchilar, S. 2011. Simulation and experimental investigation of FSP of AZ91 magnesium alloy. Materials Science and Engineering: A. 528:6469-6477. doi:10.1016/j.msea.2011.05.035.

[48] Buffa, G., Ducato, A., Fratini, L. 2013. FEM based prediction of phase transformations during Friction Stir Welding of Ti6Al4V titanium alloy. Materials Science and Engineering: A. 581:56-65. doi:10.1016/j.msea.2013.06.009.

[49] Esfandiar, M., Pourabdi, G., Akbari, M. and Eskandari, E. 2023. Numerical study and analysis of thermal parameters of subcooled flow boiling and presentation of prediction models based on artificial neural network algorithm. Karafan Quarterly Scientific Journal. 20:151-173. doi:10.48301/kssa.2023.388017.2469.

[50] Buffa, G., Hua, J., Shivpuri, R. and Fratini, L. 2006. A continuum based fem model for friction stir welding—model development. Materials Science and Engineering: A. 419:389-396. doi:10.1016/j.msea.2005.09.040.

[51] Ghangas, G., Singhal, S., Dixit, S., Goyat, V. and Kadiyan, S. 2023. Mathematical modeling and optimization of friction stir welding process parameters for armor-grade aluminium alloy. International Journal on Interactive Design and Manufacturing. 17:2323-2340. doi:10.1007/s12008-022-01000-1.

[52] Maurya, S.K., Kumar, R., Mishra, S.K., Sharma, A., Yadav, A.S. and Kar, V.R. 2022. Friction stir welding of cast aluminum alloy (A319): Effect of process parameters. Materials Today: Proceedings. 56:1024-1033. doi:10.1016/j.matpr.2022.03.271.

[53] Panwar, R. and Chandna, P. 2023. Multi-objective optimization of FSW aviation-grade AA8090 alloy: an RSM-based design approach. Aircraft Engineering and Aerospace Technology. 95:1560-1569. doi:10.1108/AEAT-12-2022-0337.

[54] Chaudhary, B., Jain, N.K. and Murugesan, J. 2022. Experimental investigation and parametric optimization of friction stir powder additive manufacturing process for aerospace-grade Al alloy. The International Journal of Advanced Manufacturing Technology. 123:603-625. doi:10.1007/s00170-022-10211-5.

[55] Abd Elnabi, M.M., El Mokadem, A. and Osman, T. 2022. Optimization of process parameters for friction stir welding of dissimilar aluminum alloys using different Taguchi arrays. The International Journal of Advanced Manufacturing Technology. 121:3935-3964. doi:10.1007/s00170-022-09531-3.

[56] Mehdi, H., Batra, L., Singh, A.P. and Malla, C. 2023. Multi-response optimization of FSW process parameters of dissimilar aluminum alloys of AA2014 and AA6061 by response surface methodology (RSM). International Journal on Interactive Design and Manufacturing. 1-16. doi:10.1007/s12008-023-01409-2.